catalysts

MDPI

Review

Recent Progress on Improving Low-Temperature Activity of Vanadia-Based Catalysts for the Selective Catalytic Reduction of NO_x with Ammonia

Zhihua Lian [1], Yingjie Li [1,2], Wenpo Shan [1,*] and Hong He [1,2,3,*]

1 Center for Excellence in Regional Atmospheric Environment and Key Laboratory of Urban Pollutant Conversion, Institute of Urban Environment, Chinese Academy of Sciences, Xiamen 361021, China; zhlian@iue.ac.cn (Z.L.); yjli@iue.ac.cn (Y.L.)
2 University of Chinese Academy of Sciences, Beijing 100049, China
3 State Key Joint Laboratory of Environment Simulation and Pollution Control, Research Center for Eco-Environmental Sciences, Chinese Academy of Sciences, Beijing 100085, China
* Correspondence: wpshan@iue.ac.cn (W.S.); honghe@rcees.ac.cn (H.H.)

Received: 31 October 2020; Accepted: 1 December 2020; Published: 4 December 2020

Abstract: Selective catalytic reduction of NO_x with NH_3 (NH_3-SCR) has been successfully applied to abate NO_x from diesel engines and coal-fired industries on a large scale. Although V_2O_5-WO_3(MoO_3)/TiO_2 catalysts have been utilized in commercial applications, novel vanadia-based catalysts have been recently developed to meet the increasing requirements for low-temperature catalytic activity. In this article, recent progress on the improvement of the low-temperature activity of vanadia-based catalysts is reviewed, including modification with metal oxides and nonmetal elements and the use of novel supports, different synthesis methods, metal vanadates and specific structures. Investigation of the NH_3-SCR reaction mechanism, especially at low temperatures, is also emphasized. Finally, for low-temperature NH_3-SCR, some suggestions are given regarding the opportunities and challenges of vanadia-based catalysts in future research.

Keywords: selective catalytic reduction; vanadia-based catalysts; low-temperature activity; reaction mechanism

1. Introduction

Nitrogen oxides (NO_x, including NO and NO_2), primarily emitted from fossil fuel combustion in both stationary and mobile sources, are major pollutants in the atmosphere. NO_x is harmful to human health and can lead to the greenhouse effect, ozone depletion, acid rain, photochemical smog, and haze. Therefore, reducing the emission of NO_x has become one of the most urgent atmospheric environment problems [1–3]. Increasingly stringent policies and legislation to control the emission of nitrogen oxides have been enacted all over the world.

In the 1970s, selective catalytic reduction of NO_x with NH_3 (NH_3-SCR) was first applied to NO_x removal from stationary sources in Japan [4], and has subsequently been widely used all over the world for NO_x control from both stationary and mobile sources [5]. The NH_3-SCR process mainly comprises the following reactions:

$$4NO(g) + 4NH_3(g) + O_2(g) \rightarrow 4N_2(g) + 6H_2O(g)$$

$$2NO_2(g) + 4NH_3(g) + O_2(g) \rightarrow 3N_2(g) + 6H_2O(g)$$

$$2NO(g) + 4NH_3(g) + 2NO_2(g) \rightarrow 4N_2(g) + 6H_2O(g)$$

$$6NO(g) + 4NH_3(g) \rightarrow 5N_2(g) + 6H_2O(g)$$

$$6NO_2(g) + 8NH_3(g) \rightarrow 7N_2(g) + 12H_2O(g)$$

Catalysts are the key components in NH_3-SCR technology for abating NO_x emission. Currently, V_2O_5-WO_3/TiO_2 is commercially applied because of its excellent catalytic performance at 300–400 °C and strong SO_2 resistance [6]. Due to the high operating temperature, the precipitator and desulfurizer units should be installed downstream of the SCR unit in power plants [7]. However, this results in deactivation of the catalysts by poisoning with heavy metals, phosphorus and alkali/alkaline earth metals existing in the stack gases. Furthermore, the flue gas temperature from steel, glass and cement plants is lower than the working temperature of traditional V-based catalysts [8]. In order to avoid rapid deactivation and the need for additional energy consumption and to satisfy increasingly stringent NO_x emission limits, the study of novel low-temperature vanadia-based SCR catalysts with high performance is highly desirable and has attracted broad attention to the deNO_x process. Figure 1 shows the numbers of papers published each year from 1991 to 2020 containing "vanadium" and "SCR" in their contents using the "web of science" search engine. The increasing trend in the number of publications reflects the popularity, importance and enthusiasm for research of the vanadia-based catalysts for NH_3-SCR.

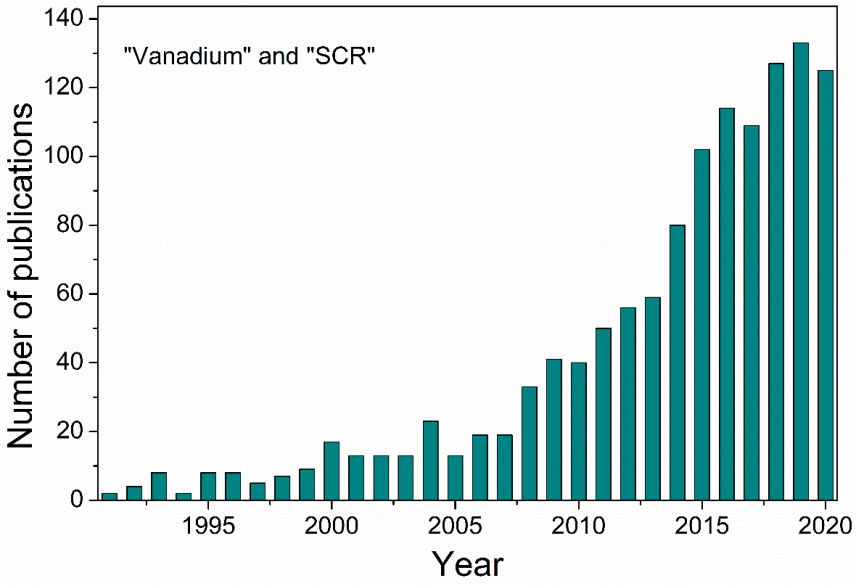

Figure 1. Number of publications on vanadia-based catalysts for NH_3-selective catalytic reduction (SCR). (Search date: 16 November 2020).

Herein, this work reviews the latest progress, especially the progress in the last five years, on vanadia-based catalysts for low-temperature NH_3-SCR, including a summary of methods for improving the performance at low temperature over vanadia-based catalysts and a discussion of the reaction mechanism of low-temperature NH_3-SCR, and finally proposes suggestions for the development of vanadia-based catalysts with superior low-temperature SCR activity.

2. Performance Improvement at Low Temperatures

The narrow operating temperature window of vanadia-based catalysts restricts their broader applications in the deNO_x process. Though catalysts with high loadings of V_2O_5 exhibit high catalytic activity, high vanadia content leads to a decrease in N_2 selectivity and thermal stability and an increase in the catalytic oxidation of sulfur dioxide to sulfur trioxide, which induces severe corrosion problems for equipment [9]. Therefore, researchers have devoted much effort to improving the low-temperature

catalytic activity of vanadia-based catalysts, including modification of the active components, supports, and preparation methods, and experimenting with metal vanadates and specific structures.

2.1. The Modification of Vanadia-Based Catalysts

There are many reports on the modification of vanadia-based catalysts with transition metal oxides or rare-earth oxides to promote low-temperature NH_3-SCR activity. V-based catalysts were modified with different transition metal (Co, Mn, Fe, Cu) oxides via the impregnation method, and Cu-V/TiO_2 was found to present the best catalytic performance at 225–375 °C, probably attributable to the increased abundance of active surface oxygen species and strong acid sites [10]. Cu-doped V_2O_5/WO_3-TiO_2 exhibited higher NO_x conversion than a V/WTi sample, which was mainly attributed to the existence of double redox couples of Cu^{2+}/Cu^{+} and V^{5+}/V^{4+} from the adjacent copper oxides and vanadium oxides on the surface [11]. In a study of the effects of different CuO doping levels, 7 wt.% Cu/VWTi exhibited high SCR activity and Hg^0 oxidation at 280–360 °C, resulting from high dispersion of active species and enhancement of the redox properties [12]. In addition, a 0.3 wt.% Ce-0.05 wt.% Cu/VWTi catalyst showed stronger K resistance and higher catalytic activity than the commercial VWTi catalyst by reason of its enhanced surface acidity and redox properties [13].

In the presence of 1000 ppm SO_2 at 280 °C, Ce-doped V/WTi showed excellent catalytic activity. An oligomeric V-O-V structure was formed on the catalyst due to the introduction of ceria, facilitating electronic conduction between the vanadia and ceria species, lowering the apparent activation energy and significantly improving the NH_3-SCR reaction performance. The stability of adsorbed NO_x species was improved, and active vanadium sites were protected from poisoning by the addition of ceria [14]. Ma et al. found that 8 wt.% CeO_2-1 wt.%V_2O_5-WO_3/TiO_2 showed higher than 80% catalytic activity at the temperature range of 190–450 °C, comparable to the performance of 3 wt.% V_2O_5-WO_3/TiO_2, showing that the usage of toxic vanadium oxides can be reduced via ceria doping in the development of low-temperature SCR catalysts [15]. Arfaoui et al. adopted a one-step sol−gel method to synthesize new sulfate and ceria co-modified V_2O_5-TiO_2 nanostructured aerogel catalysts, which presented superior catalytic performance [16]. Hu et al. reported that V-Ce$(SO_4)_2$/Ti catalysts with abundant reactive acid sites exhibited better activity than the commercial V-W/Ti catalyst and showed a strong tolerance to SO_2 and H_2O [17]. The catalysts 3Ce-V-W/TiO_2 [18], V-5W/Ce/Ti [19], $V_{0.8}WTiCe_{0.25}$ [20] and $V_1Ce_{10}Ti$ [21] all exhibited excellent SCR activity.

Chi et al. adopted an ultrasonic-assisted impregnation method to prepare Ce-Cu modified V_2O_5/TiO_2 catalysts, exhibiting high NO conversion (>97%) at 200–400 °C [22]. Xu et al. found that among TiO_2-supported vanadium oxide catalysts modified with different amounts of Ce and Sb, $V_5Ce_{35}Sb_2$/Ti presented the best SCR performance, over which 90% NO conversion was obtained at 210 °C [23]. The doping of V and Sb into Ce/Ti increased the concentration of Ce^{4+}, and V/Sb/Ce/Ti exhibited superior catalytic performance and N_2 selectivity (as shown in Figure 2) [24].

The introduction of Mn into VO_x/CeO_2 {110} can speed up the V^{5+}/V^{4+} redox cycle and increase the amount of coordinated NH_3 species and bridging nitrate species during SCR, and therefore improve the deNO_x activity [25]. Among MO_x-V_2O_5-MoO_3-CeO_2/TiO_2 (M = Mn, Cu, Sb, and La) catalysts, $Mn_5V_1Mo_3Ce_7$/Ti showed the optimal catalytic activity due to its strong reducibility and abundant acid sites with various strengths, and the tolerance of SO_2 and H_2O were enhanced remarkably by sulfate species formed in the presence of sulfur oxide [26]. V/Mo-Ti presented better NH_3-SCR performance and stronger SO_2 resistance than V/W/Ti catalysts, attributed to the greater abundance of acid sites induced by the introduction of molybdenum, and with increasing Mo^{6+} ratio, V/Mo-Ti showed increasing catalytic activity [27]. MoO_3-doped V/WTi exhibited better catalytic performance than V/WTi and 5 wt.% Mo-V/WTi presented the best deNO_x activity because the introduction of MoO_3 enhanced the amount of surface oxygen species and redox capability and altered the number, type and reaction activities of surface acid sites [28]. The doping of Cr into V/TiO_2 enhanced the low-temperature reductive capacity, increased the amounts of acid sites of weak and medium strength, and promoted the rate of the SCR reaction [29]. The optimal catalytic performance was obtained

over a 10 wt.% $Cr_{0.2}V_{0.8}/TiO_2$ catalyst. The doping of Nb_2O_5 into the V/WTi catalyst improved the low-temperature deNO_x performance, which was ascribed to the improved dispersion of vanadia and promotion of the reactivity of adsorbed ammonia species [30].

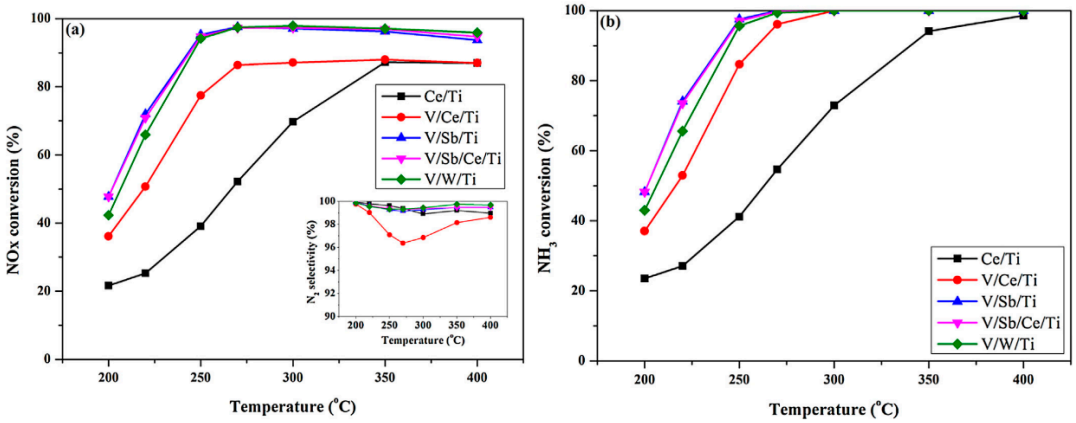

Figure 2. The effect of reaction temperature on (**a**) NO_x conversion and (**b**) NH_3 conversion of various catalysts (NO: 750 ppm, NO_2: 48 ppm, NH_3/NO_x: 1.0, O_2: 3 vol%, H_2O: 6 vol%, S.V.: 60,000 h^{-1}) [24]. Reproduced with permission from [24], copyright 2015, Elsevier.

Besides modification with metal oxides, doping with nonmetal elements can also enhance the SCR performance of the catalyst. Marberger et al. found that the doping of 2–4 wt.% SiO_2 into VW/Ti can hamper the growth of anatase crystallites at 600 and 650 °C, resulting in preservation of the low-temperature catalytic activity [31]. Zhao et al. found that the addition of N and S to V_2O_5/TiO_2 can significantly influence NH_3-SCR performance, and a catalyst with 3:1:100 (S:N:Ti) molar ratio exhibited superior performance attributed to the large pore volume and surface area, strong reducibility and increased surface acidity, electronic interactions between TiO_2 and the dispersed vanadia species, and inhibition of the anatase-to-rutile phase transformation [32,33]. The SCR activity at low temperatures was promoted evidently by the doping of F into V_2O_5/TiO_2 because modification with F promoted the interaction of vanadium species and TiO_2 by means of oxygen vacancies with electrons [34]. Liang et al. also found that F-V_2O_5-WO_3/TiO_2 could enhance the SCR activity and the resistance to sulfur and water. The surface morphology of the catalyst was eroded and the grain size was reduced by the introduction of an appropriate amount of F [35]. The introduction of a certain amount of phosphorus into V_2O_5-WO_3/TiO_2 increased the intrinsic activity for the enhancement of Lewis and Brønsted acid sites on V_2O_5-WO_3/TiO_2, and induced the formation of more polymeric surface vanadyl species through spatial effects [36]. Nam et al. added a low content of P into V/Sb/Ce/Ti, and Sb-phosphate and Ce-phosphate instead of $VOPO_4$ were formed, contributing to the enhancement of the redox properties while keeping the acidity almost unchanged, resulting in the promotion of the SCR activity [37]. A heteropoly acid (HPA)-promoted V_2O_5/TiO_2 catalyst presented better catalytic performance and stronger potassium tolerance than WO_3-promoted catalysts [38]. The modification of vanadia-based catalysts and their catalytic activity are shown in Table 1.

Table 1. Catalytic performances of vanadia-based catalysts synthesized by different methods.

Catalysts	Preparation Methods	Reaction Conditions	NO_x (or NO) Conversion (Temperature Range)	GHSV	Source
Cu-V/TiO_2	Impregnation	0.05% NO, 0.05% NH_3, 5 vol% O_2	>90% (225–375 °C)	26,000 h^{-1}	10
CuV/WTi	Impregnation	0.05% NO, 0.05% NH_3, 5 vol% O_2	>84% (250–400 °C)	10,000 h^{-1}	11
VWCeCuTi	Impregnation	0.05% NO, 0.05% NH_3, 5 vol% O_2	>80% (250–375 °C)	60,000 h^{-1}	13
V/Ce/WTi	Precipitation	0.05% NO, 0.05% NH_3, 5 vol% O_2, 5vol% H_2O	95% (250–450 °C)	18,000 h^{-1}	14
$VCeTiSO_4^{2-}$	Sol−gel	0.1% NO, 0.1% NH_3, 8 vol% O_2, 3.5vol%H_2O	>80% (275–450 °C)	120,000 h^{-1}	16
V-Ce$(SO_4)_2$/Ti	Impregnation	0.08% NO, 0.08% NH_3, 5 vol% O_2, 0.05%SO_2, 5vol%H_2O	100% (300–450 °C)	150,000 mL/g·h	17
7%Ce-1%CuV/Ti	Impregnation	0.05% NO, 0.05% NH_3, 5 vol% O_2	>97% (200–400 °C)	45,000 h^{-1}	22
$V_5Ce_{35}Sb_2/TiO_2$	Impregnation	0.1% NO, 0.1% NH_3, 3 vol% O_2	>90% (225–400 °C)	45,000 h^{-1}	23
V-Mn/Ce	Hydrothermal	0.05% NO, 0.05% NH_3, 5 vol% O_2	>80% (200–350 °C)	160,000 h^{-1}	25
V3Mo5/WTi	Impregnation	0.05% NO, 0.05% NH_3, 3 vol% O_2	>80% (200–300 °C)	60,000 h^{-1}	28
10%$Cr_{0.2}$-$V_{0.8}/TiO_2$	Impregnation	0.05% NO, 0.05% NH_3, 3 vol% O_2	>85% (160–280 °C)	60,000 mL/g·h	29
6%Nb-3% V/W-Ti	Impregnation	0.05% NO, 0.05% NH_3, 3 vol% O_2	>90% (225–400 °C)	60,000 h^{-1}	30
4%Si2%V/10%W/Ti	Co-impregnation	0.05% NO, 0.06% NH_3, 10 vol% O_2	>80% (300–500 °C)	50,000 h^{-1}	31
S_3N_1V/Ti_{100}	Sol−gel	0.05% NO, 0.05% NH_3, 5 vol% O_2	100% (240–450 °C)	27,549 h^{-1}	32
VTiF-$(NH_4)_2TiF_6$	Sol−gel	0.05% NO, 0.06% NH_3, 5 vol% O_2	78.5% (240 °C)	38,900 h^{-1}	34
0.2%F-VW/Ti	Impregnation	0.07% NO, 0.07% NH_3, 5 vol% O_2	>95% (160–360 °C)	30,000 h^{-1}	35
1P-VWTi	Impregnation	0.05% NO, 0.05% NH_3, 5 vol% O_2	96% (250 °C)	70,000 h^{-1}	36
5%V/15%TPA/Ti	Impregnation	0.1% NO, 0.1% NH_3, 4 vol% O_2 2.3 vol% H_2O	100% (300 °C)	180,000 h^{-1}	38

The improvements in low-temperature performance accomplished via modification with metal oxides or nonmetal elements were mainly related to modulation of the redox capability and acidity of the vanadia-based catalysts. Besides doping with active components, the catalyst supports were also modified to further improve the deNO_x activity.

2.2. The Effect of Different Supports

TiO_2 has been applied as a support for commercial vanadia-based catalysts for decades due to its favorable properties, including good surface dispersion of V species on TiO_2 in comparison with other supports (Al_2O_3, SiO_2, et al.) as well as weak and reversible sulfation under SCR reaction conditions [8,39,40]. However, at high reaction temperatures, anatase TiO_2 will transform to rutile TiO_2, which leads to catalyst sintering accompanied by decreases in the surface area and activity [41]. Recently, many attempts have been made to improve vanadia-based catalysts by modifying the TiO_2 support or using diverse support materials.

Vanadium oxides dispersed on microporous TiO_2 supports produced much less N_2O than commercial TiO_2-supported catalysts during the process of NH_3-SCR reaction, because the formation of bulk-like V_2O_5 species, which resulted in the formation of N_2O, was suppressed (as shown in Figure 3) [42]. The pore structure of TiO_2 determined the types of vanadium species present, which affected the sulfur resistance during the SCR reaction. A 5 wt.%V/Ti (microporous TiO_2) showed stronger resistance to sulfur poisoning and better activity than a 5 wt.%V/Ti (mesopore DT-51) having bulk-like VO_x species [43]. A catalyst with 5 wt.% vanadia ultrasonically impregnated on a TiO_2 support with a large surface area (380.5 m^2/g) had a 100 °C wider operating temperature window and higher N_2 selectivity than the traditional vanadia-based catalyst due to enhanced redox capability and total acidity [44]. Ti-bearing blast furnace slag was used to prepare the TiO_2-SiO_2 support, which was then used to support V_2O_5-WO_3 and the catalyst presented enhanced acidity and redox ability for active species and promoted the SCR activity compared with a catalyst using commercial TiO_2 as support [45]. Mixed tungsten−titanium-pillared clays were used to support vanadium oxides, and the synthesized catalysts showed a uniform distribution of WTi-pillars between the clay layers and showed good catalytic performance in NH_3-SCR [46]. Catalysts on other novel supports were also investigated, such as V_2O_5 supported on reduced TiO_2 [47], vanadium impregnated on silica-pillared layered titanate (SiO_2-Ti_4O_9) [48], supported vanadium-substituted Keggin polyoxometalates (POM) [49], V_2O_5/$H_2Ti_3O_7$-nanotubes and V_2O_5-WO_3/$H_2Ti_3O_7$-nanotubes [50], 1V4Ce/Ti-PILC (1 wt.% V and 4 wt.% Ce) [51], and V/$Ce_{1-x}Ti_x$ (x = 0.3, 0.5) [52].

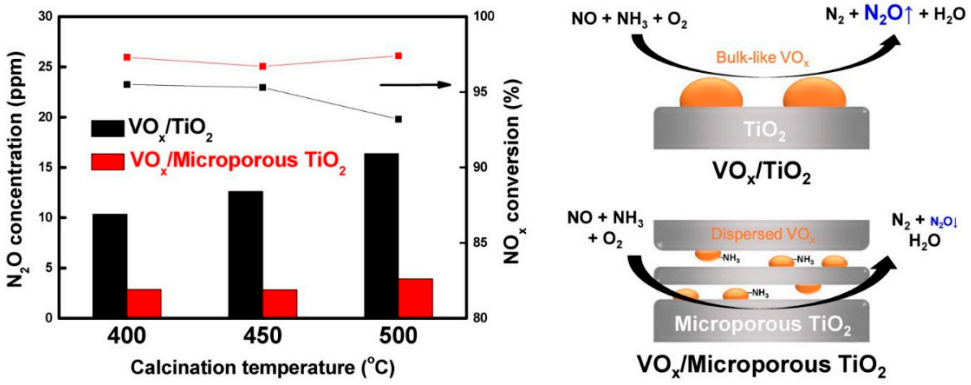

Figure 3. NO_x conversion and N_2O formation during SCR of NO with NH_3 over VO_x/DT-51 and VO_x/MP-TiO_2 calcined at various temperatures. Measurement was performed after reaching steady state in wet conditions at 400 °C [42]. Reproduced with permission from [42], copyright 2018, Elsevier.

Ce-based supports for vanadium oxide NH_3-SCR catalysts have also attracted interest. In our previous study, the homogeneous precipitation method was used to prepare vanadium oxides/CeO_2 catalysts, and the catalyst exhibited high NO_x conversion and strong tolerance to SO_2 and H_2O [53].

Incorporating Ti into V_2O_5/CeO_2 improved the NO_x conversion, N_2 selectivity and resistance to SO_2 and H_2O due to the lower crystallinity, more abundant acid sites, better dispersion of surface V species and greater number of reduced species [54]. Modification of VO_x/CeO_2 with NbO_x promoted the redox capability and acidity, leading to better NH_3-SCR activity and stronger tolerance to SO_2/H_2O than the unmodified VO_x/CeO_2 catalyst; and 30Nb-1VO_x/CeO_2 exhibited better NH_3-SCR performance than $3V_2O_5$–$10WO_3/TiO_2$ (as shown in Figure 4) [55,56].

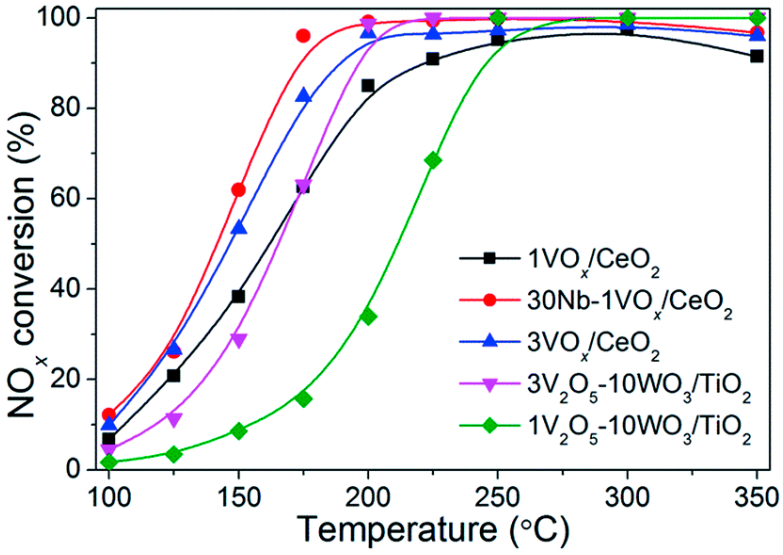

Figure 4. NH_3-SCR activity over VO_x/CeO_2 and V_2O_5-WO_3/TiO_2 catalysts [55]. Reproduced from [55], copyright 2018, Royal Society of Chemistry.

ZrO_2 supports with various morphologies (mesoporous, rod, star, sphere, hollow) were loaded with vanadium oxide, and 3 wt.% V/Zr (mesoporous) exhibited a wide operating temperature window and excellent N_2 selectivity. The content of tetravalent vanadium ions on the surface of the catalyst and catalytic performance decreased in the order of mesoporous > hollow spheres > stars > rods [57]. In addition, there are several reports on the use of Zr-modified supports such as in 5wt.%V/$Zr_{0.3}Ce_{0.7}$ [58], V/$ZrCe_{0.6}$ [59], Co-V/Zr-Ce [60], which enhanced the SCR performance of the vanadia-based catalysts. A catalyst with vanadium−tungsten oxides supported on $CuCeO_y$ microflowers showed excellent deNO_x performance at low temperatures, attributed to the facile electron transfer among V, Cu and Ce ions, decreasing the apparent activation energy of the NH_3-SCR reaction (E_a = 16.59 kJ/mol) [61]. A V/$Ce_{0.9}Fe_{0.1}$ solid solution also presented relatively high SCR activity at low temperature (below 300 °C) [62].

Carbon materials, including carbon nanotubes (CNT), carbon fibers (ACF) and activated carbon (AC), can also be used to support vanadia-based catalysts for NH_3-SCR for large specific surface area and pore volume. Carbon nanotube-supported vanadium oxide (V_2O_5/CNT) exhibited high NO reduction activity and high stability at low-temperatures, and the activity in the presence of sulfur dioxides was significantly promoted [63]. Sulfur dioxide could enhance the catalytic activity of a V_2O_5/SiC catalyst at 250 °C because pre-adsorption with SO_2 + O_2 enhanced NH_3 adsorption and at low temperatures, NO could effectively react with the ammonium bisulfate that was formed on the surface of the catalyst [64]. Excellent SCR performance and SO_2 resistance were also achieved by 3 wt.%Fe-0.5 wt.%V/AC [65], and Mn-Ce-V/AC [66].

Improving the properties of the support could thus improve the dispersion of vanadium species and the interaction between the support and active components, enhance electron transfer between active components, enlarge the specific surface area, and strengthen the redox capability and acidity, all of which are beneficial to accelerating the SCR reaction.

2.3. The Effect of Preparation Method

The preparation methods utilized for catalysts mainly include the precipitation method, sol−gel method, hydrothermal method, impregnation method, and other specialized synthesis methods. Different synthesis methods and synthesis parameters influence the nanostructures, morphologies, and surface physicochemical properties, finally affecting the NH_3-SCR catalytic activity. Hence, it is important to optimize the synthesis method to improve the NH_3-SCR activity over vanadia-based catalysts.

Compared to materials prepared by incipient wetness impregnation, coprecipitated V_2O_5-WO_3/TiO_2 catalysts presented superior SCR performance derived from their increased ammonia adsorption capacity due to the existence of new surface WO_x site-associated surface defects on the TiO_2 support [67]. A V/Ce/WTi-DP (deposition precipitation) catalyst exhibited more O_α, stronger reducibility and more surface Ce species, thus showing less N_2O formation and better medium-temperature NH_3-SCR performance than similar catalysts prepared by impregnation [68]. CeO_2-modified V_2O_5/TiO_2 synthesized via chemical vapor condensation exhibited a higher ratio of Ce^{3+} and showed higher reducibility and acidity than that synthesized by the impregnation method [69]. In our previous work, VO_x/CeO_2 synthesized via the homogeneous precipitation method presented better catalytic performance and stronger tolerance to H_2O and SO_2 than that synthesized via sol−gel method, incipient wetness impregnation and rotary evaporation impregnation, which can be ascribed to the lower crystallinity of CeO_2 on the surface, greater abundance of acid sites and vanadium species, and better dispersion of V species [53]. The support synthesis methods had an effect on structure and performance of VO_x/CeO_2 catalysts, and the catalyst from precipitation method prepared-support was more active than that from citrate method due to higher surface area and a more effective incorporation of V sites into the support surface [70]. A series of VWTi nanoparticle catalysts were directly synthesized via the sol−gel method, and $V_{0.02}W_{0.04}Ti$ showed the best SCR activity and the lowest apparent activation energy due to a high concentration of distorted and reducible vanadium species [71].

Besides these conventional synthesis methods, several novel preparation methods were developed to enhance catalytic activity of vanadia-based NH_3-SCR catalysts. Chen et al. prepared $V_{0.1}Ti_{0.9}O_{2-\delta}$ catalysts by flame synthesis with promoted low-temperature activity due to strong redox properties, and different synthesis conditions also effected the properties of the catalysts and their catalytic activity [72]. Arfaoui prepared a V_2O_5-CeO_2-TiO_2-SO_4^{2-} nanostructured aerogel catalyst via a one-step sol−gel method accompanied by the supercritical drying process, which presented a large surface area (66 m^2/g), large porosity and good thermal stability [16]. Tuning the interaction degree supplied by external forces can regulate the morphology. Rotation-assisted hydrothermal synthesis can be used to prepare thick multiwalled titanate nanotubes and when used as the support for vanadium−tungsten-oxide, the resulting catalysts presented stable catalytic activity because the sintering of VO_x was suppressed by the multiwalled nanotubes [73]. Doronkin et al. found that V/Ti and V-W/Ti catalysts prepared via incipient wetness impregnation and grafting with highly dispersed, isolated and polymeric V-oxo species exhibited high SCR activity [74].

In the synthesis of catalysts, different preparation parameters can also affect the physicochemical properties and the catalytic activity. For example, different vanadium precursors have an influence on the dispersion of V species and catalytic performance [75]. V_2O_5/TNTs catalysts prepared using $VOSO_4$ as the V precursor exhibited stronger synergistic effects with the TNTs than those made with a NH_4VO_3 precursor, and active metal precursors containing cation groups were superior to those with anion groups (as shown in Figure 5) [76]. During the preparation process of iron vanadate, the pH value determined the stoichiometry of the $FeVO_4$/TiO_2-WO_3-SiO_2 product: vanadium-rich samples were prepared at pH lower than 6, stoichiometric $FeVO_4$ was obtained in the pH range of 4–6, while samples prepared at pH > 6 were rich in Fe_2O_3 [77]. The NH_3 adsorption capacity of Ce-doped V_2O_5-WO_3/TiO_2 was affected by the sequence of impregnation by Ce and W, and 0.2V-5W-5Ce/Ti exhibited stronger SO_2 and H_2O tolerance than 0.2V-(5Ce5W)/Ti and 0.2V-5Ce-5W/Ti [78]. Compared to the untreated

sample, V-Ce-Ni/TiO_2 catalysts treated by nonthermal plasma possessed smaller particle size, better dispersion and more uniform distribution of active sites, as well as larger number of oxygen vacancy and acid sites. Therefore, the plasma-treated catalysts showed improved catalytic performance at low temperatures with a wider operating temperature window [79]. Moreover, the treatment atmosphere can also have an influence on catalytic performance. The ratios of active polymeric V-O-V species and further NH_3-SCR activity decreased in the following order: V/Ti > V/Ti-O_2 > V/Ti-N_2 > V/Ti-NH_3 [80].

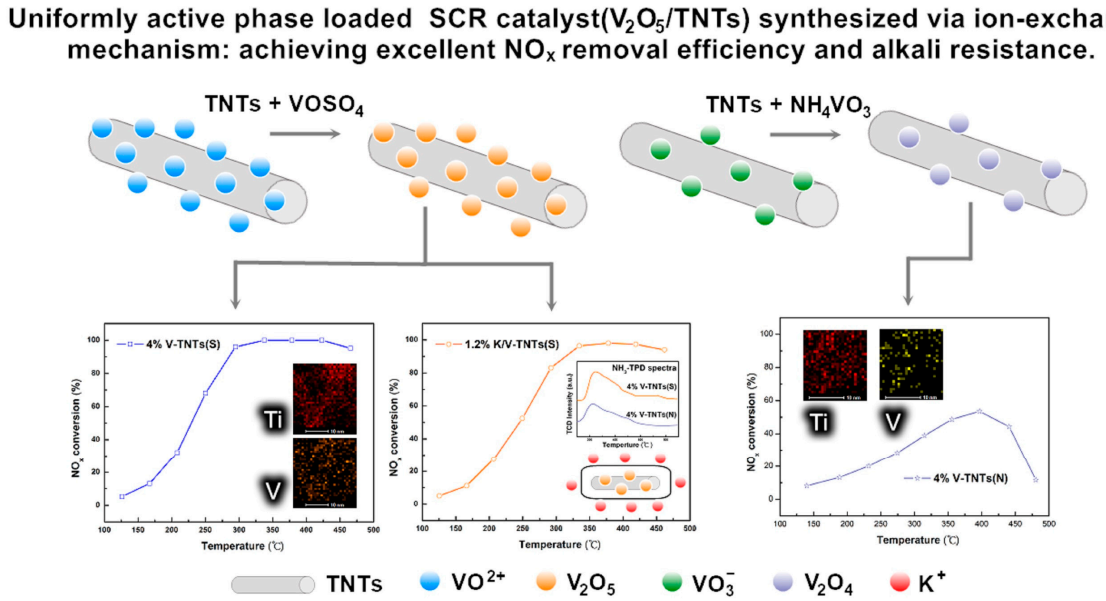

Figure 5. SCR catalysts (V_2O_5/TNTs) uniformly loaded with active phase synthesized via ion-exchange mechanism [76]. Reproduced with permission from [76], copyright 2018, Elsevier.

2.4. Metal Vanadates

Although vanadia-based catalysts show superior catalytic performance at medium temperatures and have been widely applied in the deNO_x process, the volatility and the toxicity of vanadium oxide at high temperature is a crucial problem. However, metal vanadates present better thermal stability than V_2O_5 due to their higher melting points (e.g., 780, 850, 1030 and 1100 °C for copper vanadate, iron vanadate, manganese vanadate and cerium vanadate, respectively). Therefore, metal vanadates can be candidates for vanadia-based catalysts with great potential [81].

Iron vanadates ($FeVO_4$) have recently been extensively studied as active NH_3-SCR catalysts. Abundant surface defects existed on a $FeVO_4$/TiO_2 catalyst for the adsorption and activation of reactants, and the true active sites were $FeVO_4$ phase surface-enriched with VO_x species. Thus, similar to V_2O_5/TiO_2, $FeVO_4$/TiO_2 showed superior catalytic performance and H_2O/SO_2 tolerance [1]. $Fe_{0.75}V_{0.25}O_\delta$ exhibited excellent SCR performance in the temperature range of 175–400 °C. It was found that the formation of amorphous $FeVO_4$ resulted from the incorporation of V into Fe_2O_3, and the apparent activation energy decreased due to the synergistic effect of $FeVO_4$ and Fe_2O_3 improving the catalytic activity at low temperatures [82]. Due to the greater electronic inductive effect, $Fe_2V_4O_{13}$/TiO_2 showed stronger redox capability and more sites accessible to NO_x/NH_3 than $FeVO_4$/TiO_2 and thus presented higher activity in the presence of H_2O [83].

Marberger et al. found that compared to the 2.3 wt.% V_2O_5/TiO_2-WO_3-SiO_2 catalyst, 4.5 wt.% $FeVO_4$/TiO_2-WO_3-SiO_2 showed enhanced catalytic performance, and the decomposition of $FeVO_4$ led to an activation effect due to the dispersal and migration of VO_x species to the surface of the support material, which were the active species responsible for NH_3-SCR [84]. Wu et al. proposed that the performance of $FeVO_4$/TiO_2-WO_3-SiO_2 was structure-sensitive, and that the pH values adopted during the preparation process had an influence on the nanostructure and morphology. The optimal catalyst showed 90% NO_x conversion in the temperature range of 246–476 °C and strong tolerance to SO_2 and

H_2O [85]. The doping of Er into $FeVO_4$/TiWSi could block the transformation to rutile, inhibiting the deactivation of $FeVO_4$ due to thermal aging and thus improving the activity after thermal treatment, and the Fe loading determined the medium/low-temperature catalytic activity. $Fe_{0.5}Er_{0.5}VO_4$ was found to exhibit superior catalytic performance and stability [86].

The oxidation of NO to NO_2 was enhanced by the coexistence of Ce^{4+} species stabilized as CeO_2 with bulk $CeVO_4$. Aging treatments under wet atmosphere at 500 and 600 °C did not result in the sublimation and loss of vanadium [87]. The introduction of Zr into $CeVO_4$ to form a $Ce_{1-x}Zr_xVO_4$ solid solution led to high activity, with a 125 °C light-off temperature and a wide temperature window of 150–375 °C by reason of the increased surface area, surface active oxygen species and acid sites of the catalysts [81]. Zr-$CeVO_4$/TiO_2-nanosheets showed better SCR performance, stability and tolerance to H_2O/SO_2 than nanoparticles due to their more abundant Brønsted acid sites and active oxygen species [88]. A catalyst with Ce:V = 1:1 supported on sulfated zirconia showed high activity in the presence of SO_2 and potassium. The incorporation of vanadium led to the formation of $CeVO_4$, preventing reaction between SO_2 and CeO_2 and maintaining the reactivity of active sites, thus enhancing the tolerance toward SO_2 [89]. The doping of Sn into $CeVO_4$ catalysts can broaden the temperature window and improve the resistance to SO_2 and H_2O, mainly resulting from the large specific surface area (from 40.75 to 49.05 m^2/g), strong interactions among vanadium, cerium and tin, and large numbers of oxygen vacancies and acid sites [90].

Compared to CuV_2O_6 (Cu_1/Ti), $Cu_2V_2O_7$ (Cu_2/Ti), and $Cu_3V_2O_8$ (Cu_3/Ti), $Cu_5V_2O_{10}$ (Cu_5/Ti) presented optimal redox behavior and the largest number of acid sites, and therefore presented the greatest SCR performance at low temperatures [91]. The addition of Sb as a promoter can further improve the SCR activity over copper vanadate catalysts due to the improved redox properties [91]. SO_2 and O_2 can be used to modify Sb-promoted $Cu_3V_2O_8$ on TiO_2, and 400 °C was an adequate functionalization temperature to promote the redox behavior and increase the number of Brønsted acid sites, resulting from the more abundant surface $Cu(SO_4)$ or from a proper combination of the metal-bound SO_Y^{2-} species with monodentate and bidentate binding configurations, to enhance the catalytic performance (as shown in Figure 6) [92].

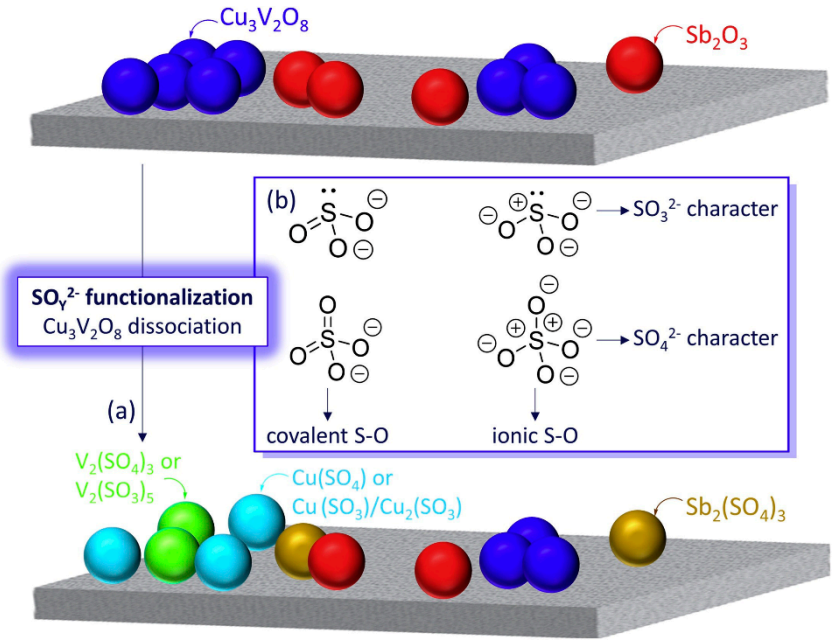

Figure 6. Schematic representation of Cu_3-$Sb_{1.4}$/TiO_2 surface prior to and post SO_Y^{2-} functionalization. (**a**) Change in the surface species upon SO_Y^{2-} functionalization to potentially dissociate the $Cu_3V_2O_8$ particles and generate V, Cu, or Sb-based sulffite or sulfate species. (**b**) Covalent or ionic characters of the S-O bonds possibly inherent to the metal-SO_Y^{2-} species [92]. Reproduced with permission from [92], copyright 2019, Elsevier.

In summary, metal vanadates can not only increase the low/medium-temperature NH_3-SCR activity but also enhance the thermal stability [93,94]. The metal vanadates have aroused the interest of researchers due to their excellent chemical and physical properties. In future studies, the metal vanadate can obtain higher SCR activity through doping different elements or changing the preparation methods, etc.

2.5. Specific Structures

Tuning the structure and morphology of nanoparticle catalysts can enhance the NH_3-SCR activity. Thus, researchers have made great efforts to regulate the structure and morphology of vanadia-based catalysts. A $FeVO_4$ nanorod/TiO_2 monolith catalyst exhibited a remarkably higher catalytic activity than a traditional $FeVO_4$ nanoparticle/TiO_2 catalyst, due to the predominantly exposed reactive planes (−210) contributing to the stronger redox capability and more abundant surface active oxygen species [95]. Multichannel TiO_2 nanotubes can provide abundant surface-adsorbed oxygen species and anchor active components efficiently, and a CeVTi-nanotube catalyst presented satisfactory NH_3-SCR activity in the temperature range of 220–460 °C [96]. Bulk TiO_2 was treated by a hydrothermal reaction to obtain zeolitic microporous TiO_2 to support vanadia-based catalysts, and compared to conventional V_2O_5/TiO_2, the catalyst not only maintained excellent SCR performance but also suppressed N_2O emission significantly [97]. V/CeO_2 nanopolyhedrons showed better SCR activity than nanocubes and nanorods for their abundant surface acid sites and appropriate redox ability (as shown in Figure 7) [98]. TiO_2 with different crystal types was used to support 3 wt.%V_2O_5, and the catalytic activity was found to depend on the dominant crystal facets of the TiO_2 nanoparticles. V_2O_5 loaded onto sheet-like TiO_2, on which anatase (001) facets were preferentially exposed, presented a better catalytic performance than that loaded onto commercial TiO_2 (TiO_2-P25) or octahedral TiO_2 with preferentially exposed anatase (101) facets, as the catalyst presented larger amounts of chemisorbed oxygen and better dispersion and stronger reducibility of V species [99]. A titania nanotube-encapsulated vanadium oxide catalyst exhibited a monolayer of isolated species where V^{5+} was the dominant oxidation state and demonstrated a wide operating temperature window, which was due to the active species being well dispersed on the support surface [100].

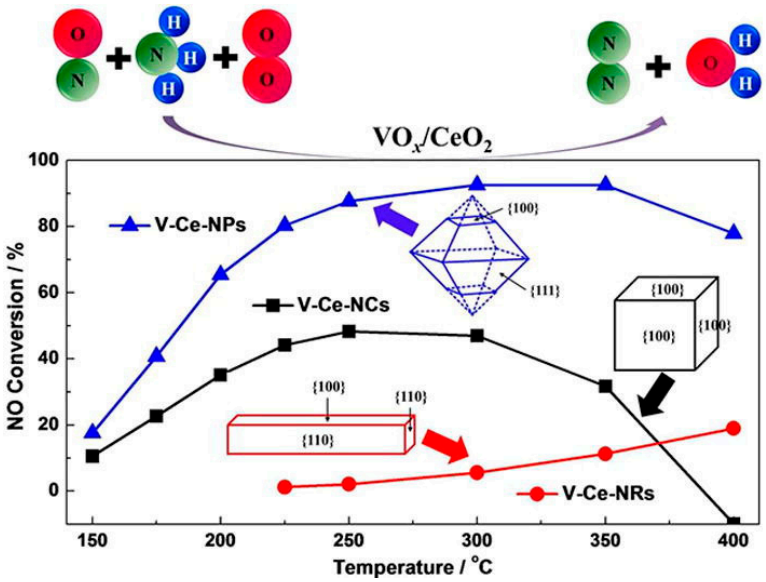

Figure 7. NO conversion as a function of temperature in the NH_3-SCR reaction [98]. Reproduced with permission from [98], copyright 2018, Elsevier.

3. Reaction Mechanism at Low Temperatures

Although vanadia-based NH_3-SCR catalysts have been commercialized for decades, the reaction mechanism on the catalysts has still been a focus of research in recent years, including the identification of active sites and intermediates and elucidation of the interaction of the active sites with the reactants. The NH_3-SCR reaction pathway proceeds as follows: the adsorbed NH_3 species react either with adsorbed nitrites/nitrates (Langmuir−Hinshelwood mechanism, i.e., L–H) or directly with gaseous NO (Eley−Rideal mechanism, i.e., E–R) to generate intermediates that subsequently decompose to N_2 and H_2O [5,101,102]. The acid sites and redox sites work together in the NH_3-SCR reaction on the catalysts, and the close coupling of acid and redox sites is a design principle for SCR catalysts with excellent NO_x purification efficiency [103].

In a debating issue about the active sites of NH_3-SCR on VWTi catalysts, it has been reported before that both surface $NH_4^+{}_{,ads}$ and $NH_{3,ads}$ participated in the NH_3-SCR reaction and the coverage of surface tungsten and vanadia oxide species, moisture, and temperature determined their relative population [104]. The large amount of surface $NH_4^+{}_{,ads}$ intermediates present a lower specific SCR activity (TOF) than the minority surface $NH_{3,ads}$ intermediates. The SCR reaction rate does not depend on the exposed Ti^{4+} sites on the support. Marberger et al. [105] proposed that NO reacts predominantly with coordinated NH_3 adsorbed on Lewis acid sites consisting of isolated V^{5+} which were reduced only in the coexistence of NH_3 and NO, and the reduction of V^{5+} was accompanied by the formation of a nitrosamide intermediate at low temperature. Brønsted acid sites, serving as an NH_3 pool and hardly contributing to the NH_3-SCR reaction, can replenish the Lewis acid sites. The rate-determining step is re-oxidation and regeneration of active Lewis acid sites.

The presence of H_2O and changes in the redox state of vanadia-based catalysts led to a reversible change between Brønsted and Lewis acid sites. Under reducing conditions, the surface was enriched with Lewis acid sites because that ammonia could be coordinated on the reduced vanadium sites as supplementary of Lewis acid sites, while more abundant Brønsted acid sites on the V/Ti catalyst surface were generated under an oxidizing environment [106]. Brønsted acid sites are important at low temperatures, while Lewis acid sites dominate the overall reaction at high temperatures. Lewis acid sites can transform to Brønsted acid sites at temperatures above 300 °C through hydrogen migration [107]. The number of Lewis acid sites decreased and the amount of Brønsted acid sites increased with changes in the vanadium content. The increase of vanadium pentoxide loading resulted in the increase of the amount of V-OH in polymeric vanadyl and the decrease of the amount of isolated vanadyl (V=O) species [108].

Most current investigations of the NH_3-SCR reaction process over V-based catalysts have mainly concentrated on isolated monomeric vanadyl species, while the polymerization of vanadium species and the coupling effects were not taken into consideration. In our previous study [109], DFT calculations were carried out to elucidate the differences between the NH_3-SCR mechanisms taking place on polymeric and monomeric vanadyl species at atomic scale. The results showed that NH_3 adsorbed on surface Ti sites transfered a hydrogen atom to the vanadyl species firstly and then reacted with gaseous NO according to the Eley−Rideal mechanism. An NH_2NO intermediate and a V-OH or V-OH_2 group were formed and then N_2 and H_2O were generated from the decomposition of NH_2NO. The consumed surface oxygen on the vanadyl species was replenished by gas-phase O_2. The catalytic cycle was completed when V=O groups were regenerated (as shown in Figure 8).

For the monomeric vanadyl species, a VOOH intermediate was formed after the transfer of an H atom of the adsorbed NH_3 to the adsorbed O_2 on vanadyl species and rapidly transformed into O=V-OH. However, for polymeric vanadyl species, the thermal stability and lifetime of the VOOH intermediate were enhanced because a hydrogen bond was formed between VOOH and the adjacent V=O group. Therefore, on polymeric vanadyl species, the VOOH intermediate can easily react with NO. The overall reaction barrier of the catalytic cycle decreases and the reaction pathway for the regeneration of redox sites is shortened due to the coupling effect of polymeric vanadyl species. Therefore, the NH_3-SCR reaction rate is significantly enhanced on polymeric species.

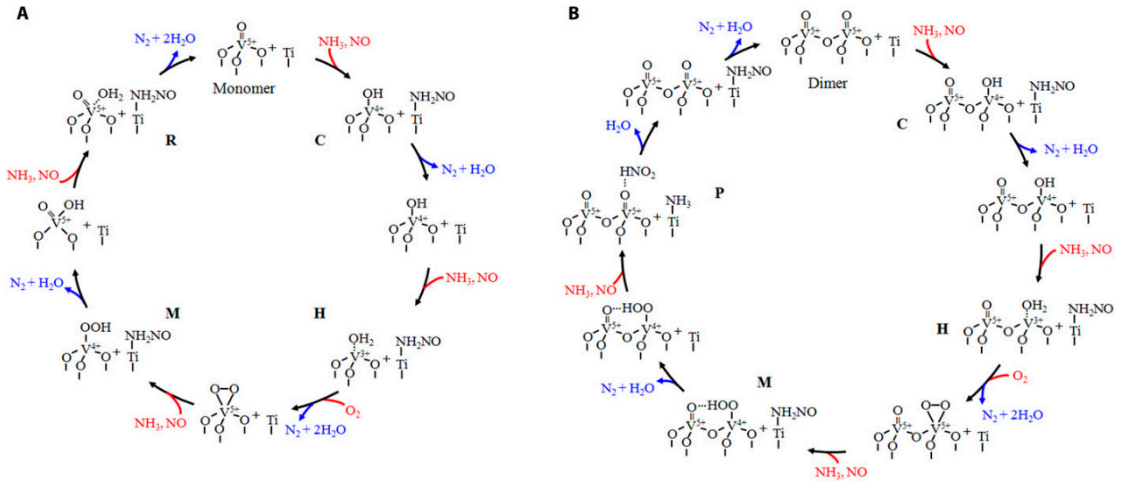

Figure 8. Mechanism of the standard NH_3-SCR reaction. (**A**) Reactions over monomeric vanadia/TiO_2 surfaces. (**B**) Reactions over dimeric vanadia/TiO_2 surfaces. Reactants are marked in red, and products are marked in blue [109]. Reproduced from [109], copyright 2018, American Association for the Advancement of Science.

Jaegers et al. clarified that the formation of oligomeric vanadia structures on supported V_2O_5-WO_3/TiO_2 was promoted by the unreactive surface tungsten oxide (WO_3), revealing a 2-site mechanism due to the presence of a proportional relationship of SCR reaction rate to the square of surface VO_x concentration. The enhancement of the NH_3-SCR reaction from the incorporation of a promoter occurs via a structural effect generated by adjacent surface sites rather than an electronic effect [110].

The presence of H_2O can have an influence on the reaction pathway for NH_3-SCR at low temperatures. In the standard and fast SCR reactions, adsorbed NH_3 reacts with nitrite species to generate N_2 and H_2O (nitrite path), while the reaction between gaseous NO and NH_4NO_3 formed from adsorbed ammonia species and surface nitrates to emit NO_2, H_2O and N_2 (NH_4NO_3 path) does not occur at low temperatures without H_2O, and in the presence of H_2O both the "nitrite path" and the "NH_4NO_3 path" contribute to the NH_3-SCR reaction [111].

For vanadia-based catalysts, different NH_3-SCR reaction pathways occur on various vanadium species. The reaction mechanism can be more complicated over modified vanadia-based catalysts and is also related to the concentration of vanadium oxide and the reaction temperature. Therefore, a variety of modern characterization and computational techniques should be applied in order to have a better view of the NH_3-SCR reaction mechanism, guiding the design of excellent deNO_x catalysts.

4. Conclusions and Perspective

Commercial V_2O_5-WO_3/TiO_2 catalysts have been widely applied for abating nitrogen oxides from mobile and stationary sources. However, the poor low-temperature activity of vanadia-based catalysts restricts their broader application in the process of NO_x purification. Therefore, this review summarizes the latest research progress on the improvement of deNO_x performance over vanadia-based catalysts at low temperatures and the NH_3-SCR reaction mechanism, and outlines opportunities and challenges for vanadia-based catalysts in the near future.

The NH_3-SCR catalytic performance over vanadia-based catalysts at low temperatures is mainly determined by polymeric vanadyl species, while monomeric species presented lower catalytic activity. The NH_3-SCR reaction needs acid sites and redox sites to work together. The good dispersion of sites with the same function and close coupling of sites with different functions are crucial for the design of excellent NH_3-SCR catalysts. However, considering the complexity of the SCR reaction, the NH_3-SCR reaction mechanisms and the structure−activity relationships still need to be investigated in-depth to gain an enhanced understanding and thus improve catalyst design theory. Furthermore, due to the

multielement composition of the developed catalysts, the synergistic reaction mechanisms between different active components, additive and diverse supports need in-depth exploration.

The modification of vanadia-based catalysts with metal oxides or nonmetal elements can improve the low-temperature SCR activity effectively. Diverse supports have been used to improve the dispersion of vanadium oxide and the interaction between the supports and the active components. The utilization of different preparation methods and use of metal vanadates and specific structures can also promote the catalytic performance of vanadia-based catalysts at low temperatures. Though great progress has been made recently, the catalysts still face many challenges in practical application, such as alkali poisoning and halogen poisoning. We need to develop catalysts with better performance to deal with the practical problems with superior low-temperature activity, wide operation windows, strong mechanical and thermal stability, and excellent resistance to alkali, heavy-metal, SO_2, and P/HCl poisoning. However, due to the volatility and toxicity of vanadium oxide, in the future catalysts with a low loading of vanadium or even no vanadium may be the main development trend in the field of NO_x removal.

Funding: This work was supported by the National Natural Science Foundation of China (21637005 and 51822811) and the Strategic Priority Research Program of the Chinese Academy of Sciences (XDA23010201).

Conflicts of Interest: The authors declare no conflict of interest.

References

1. Liu, F.; He, H.; Lian, Z.; Shan, W.; Xie, L.; Asakura, K.; Yang, W.; Deng, H. Highly dispersed iron vanadate catalyst supported on TiO_2 for the selective catalytic reduction of NO_x with NH_3. *J. Catal.* **2013**, *307*, 340–351. [CrossRef]
2. Baiker, A.; Dollenmeier, P.; Glinski, M.; Reller, A. Selective catalytic reduction of nitric oxide with ammonia: II. Monolayers of vanadia immobilized on titania-silica mixed gels. *Appl. Catal.* **1987**, *35*, 365–380. [CrossRef]
3. Baiker, A.; Dollenmeier, P.; Glinski, M.; Reller, A. Selective catalytic reduction of nitric oxide with ammonia: I. Monolayer and multilayers of vanadia supported on titania. *Appl. Catal.* **1987**, *35*, 351–364. [CrossRef]
4. Rosenberg, H.S.; Curran, L.M.; Slack, A.V.; Ando, J.; Oxley, J.H.J.P.i.E.; Science, C. Post combustion methods for control of NO_x emissions. *Prog. Energy Combust. Sci.* **1980**, *6*, 287–302. [CrossRef]
5. Busca, G.; Lietti, L.; Ramis, G.; Berti, F. Chemical and mechanistic aspects of the selective catalytic reduction of NO_x by ammonia over oxide catalysts: A review. *Appl. Catal. B* **1998**, *18*, 1–36. [CrossRef]
6. Lai, J.K.; Wachs, I.E. A perspective on the selective catalytic reduction (SCR) of NO with NH_3 by supported V_2O_5-WO_3/TiO_2 catalysts. *ACS Catal.* **2018**, *8*, 6537–6551. [CrossRef]
7. Han, L.; Cai, S.; Gao, M.; Hasegawa, J.Y.; Wang, P.; Zhang, J.; Shi, L.; Zhang, D. Selective catalytic reduction of NO_x with NH_3 by using novel catalysts: State of the art and future prospects. *Chem. Rev.* **2019**, *119*, 10916–10976. [CrossRef]
8. Xu, J.; Chen, G.; Guo, F.; Xie, J. Development of wide-temperature vanadium-based catalysts for selective catalytic reducing of NO_x with ammonia: Review. *Chem. Eng. J.* **2018**, *353*, 507–518. [CrossRef]
9. Kobayashi, M.; Kuma, R.; Masaki, S.; Sugishima, N. TiO_2-SiO_2 and V_2O_5/TiO_2-SiO_2 catalyst: Physico-chemical characteristics and catalytic behavior in selective catalytic reduction of NO by NH_3. *Appl. Catal. B* **2005**, *60*, 173–179. [CrossRef]
10. Zhao, X.; Huang, L.; Li, H.; Hu, H.; Han, J.; Shi, L.; Zhang, D. Highly dispersed V_2O_5/TiO_2 modified with transition metals (Cu, Fe, Mn, Co) as efficient catalysts for the selective reduction of NO with NH_3. *Chin. J. Catal.* **2015**, *36*, 1886–1899. [CrossRef]
11. Shen, M.; Li, C.; Wang, J.; Xu, L.; Wang, W.; Wang, J. New insight into the promotion effect of Cu doped V_2O_5/WO_3-TiO_2 for low temperature NH_3-SCR performance. *RSC Adv.* **2015**, *5*, 35155–35165. [CrossRef]
12. Wang, H.; Wang, B.; Zhou, J.; Li, G.; Zhang, D.; Ma, Z.; Xiong, R.; Sun, Q.; Xu, W.Q. CuO modified vanadium-based SCR catalysts for Hg^0 oxidation and NO reduction. *J. Environ. Manag.* **2019**, *239*, 17–22. [CrossRef] [PubMed]
13. Li, H.; Miao, J.; Su, Q.; Yu, Y.; Chen, Y.; Chen, J.; Wang, J. Improvement in alkali metal resistance of commercial V_2O_5-WO_3/TiO_2 SCR catalysts modified by Ce and Cu. *J. Mater. Sci.* **2019**, *54*, 14707–14719. [CrossRef]

14. Li, C.; Shen, M.; Wang, J.; Wang, J.; Zhai, Y. New insights into the promotional mechanism of ceria for activity and ammonium bisulfate resistance over V/WTi catalyst for selective catalytic reduction of NO with NH_3. *Appl. Catal. A* **2018**, *560*, 153–164. [CrossRef]
15. Ma, Z.; Wu, X.; Feng, Y.; Si, Z.; Weng, D.; Shi, L. Low-temperature SCR activity and SO_2 deactivation mechanism of Ce-modified V_2O_5-WO_3/TiO_2 catalyst. *Prog. Nat. Sci. Mater. Int.* **2015**, *25*, 342–352. [CrossRef]
16. Arfaoui, J.; Ghorbel, A.; Petitto, C.; Delahay, G. Novel V_2O_5-CeO_2-TiO_2-SO_4^{2-} nanostructured aerogel catalyst for the low temperature selective catalytic reduction of NO by NH_3 in excess O_2. *Appl. Catal. B* **2018**, *224*, 264–275. [CrossRef]
17. Hu, W.; Zhang, Y.; Liu, S.; Zheng, C.; Gao, X.; Nova, I.; Tronconi, E. Improvement in activity and alkali resistance of a novel V-Ce$(SO_4)_2$/Ti catalyst for selective catalytic reduction of NO with NH_3. *Appl. Catal. B* **2017**, *206*, 449–460. [CrossRef]
18. Liang, Q.; Li, J.; He, H.; Liang, W.; Zhang, T.; Fan, X. Effects of SO_2 on the low temperature selective catalytic reduction of NO by NH_3 over CeO_2-V_2O_5-WO_3/TiO_2 catalysts. *Front. Environ. Sci. Eng.* **2017**, *11*, 4. [CrossRef]
19. Li, C.; Shen, M.; Wang, J.; Wang, J.; Zhai, Y. New insights into the role of WO_3 in improved activity and ammonium bisulfate resistance for NO reduction with NH_3 over V-W/Ce/Ti catalyst. *Ind. Eng. Chem. Res.* **2018**, *57*, 8424–8435. [CrossRef]
20. Zhao, L.; Li, C.; Zhang, J.; Zhang, X.; Zhan, F.; Ma, J.; Xie, Y.; Zeng, G. Promotional effect of CeO_2 modified support on V_2O_5-WO_3/TiO_2 catalyst for elemental mercury oxidation in simulated coal-fired flue gas. *Fuel* **2015**, *153*, 361–369. [CrossRef]
21. Wu, S.; Yao, X.; Zhang, L.; Cao, Y.; Zou, W.; Li, L.; Ma, K.; Tang, C.; Gao, F.; Dong, L. Improved low temperature NH_3-SCR performance of FeMnTiO_x mixed oxide with CTAB-assisted synthesis. *Chem. Commun.* **2015**, *51*, 3470–3473. [CrossRef] [PubMed]
22. Chi, G.; Shen, B.; Yu, R.; He, C.; Zhang, X. Simultaneous removal of NO and Hg^0 over Ce-Cu modified V_2O_5/TiO_2 based commercial SCR catalysts. *J. Hazard. Mater.* **2017**, *330*, 83–92. [CrossRef] [PubMed]
23. Ku, C.; Liu, J.; Zhao, Z.; Yu, F.; Cheng, K.; Wei, Y.; Duan, A.; Jiang, G. NH_3-SCR denitration catalyst performance over vanadium-titanium with the addition of Ce and Sb. *J. Environ. Sci.* **2015**, *31*, 74–80.
24. Kwon, D.W.; Nam, K.B.; Hong, S.C. The role of ceria on the activity and SO_2 resistance of catalysts for the selective catalytic reduction of NO_x by NH_3. *Appl. Catal. B* **2015**, *166*, 37–44. [CrossRef]
25. Wu, X.; Yu, X.; Huang, Z.; Shen, H.; Jing, G. MnO_x-decorated VO_x/CeO_2 catalysts with preferentially exposed {110} facets for selective catalytic reduction of NO_x by NH_3. *Appl. Catal. B* **2020**, *268*, 118419. [CrossRef]
26. Zhang, D.; Ma, Z.; Wang, B.; Sun, Q.; Xu, W.; Zhu, T. Effects of MO_x (M=Mn, Cu, Sb, La) on V-Mo-Ce/Ti selective catalytic reduction catalysts. *J. Rare Earths* **2020**, *38*, 157–166. [CrossRef]
27. Kwon, D.W.; Park, K.H.; Ha, H.P.; Hong, S.C. The role of molybdenum on the enhanced performance and SO_2 resistance of V/Mo-Ti catalysts for NH_3-SCR. *Appl. Surf. Sci.* **2019**, *481*, 1167–1177. [CrossRef]
28. Zhu, L.; Zhong, Z.; Yang, H.; Wang, C. Effect of MoO_3 on vanadium based catalysts for the selective catalytic reduction of NO_x with NH_3 at low temperature. *J. Environ. Sci.* **2017**, *56*, 169–179. [CrossRef]
29. Yang, R.; Huang, H.F.; Chen, Y.J.; Zhang, X.X.; Lu, H.F. Performance of Cr-doped vanadia/titania catalysts for low-temperature selective catalytic reduction of NO_x with NH_3. *Chin. J. Catal.* **2015**, *36*, 1256–1262. [CrossRef]
30. Zhu, L.; Zhong, Z.; Xue, J.; Xu, Y.; Wang, C.; Wang, L. NH_3-SCR performance and the resistance to SO_2 for Nb doped vanadium based catalyst at low temperatures. *J. Environ. Sci.* **2018**, *65*, 306–316. [CrossRef]
31. Marberger, A.; Ferri, D.; Rentsch, D.; Krumeich, F.; Elsener, M.; Krocher, O. Effect of SiO_2 on co-impregnated V_2O_5/WO_3/TiO_2 catalysts for the selective catalytic reduction of NO with NH_3. *Catal. Today* **2019**, *320*, 123–132. [CrossRef]
32. Zhao, W.; Dou, S.; Zhang, K.; Wu, L.; Wang, Q.; Shang, D.; Zhong, Q. Promotion effect of S and N co-addition on the catalytic performance of V_2O_5/TiO_2 for NH_3-SCR of NO_x. *Chem. Eng. J.* **2019**, *364*, 401–409. [CrossRef]
33. Zhao, W.; Zhong, Q.; Pan, Y.; Zhang, R. Systematic effects of S-doping on the activity of V_2O_5/TiO_2 catalyst for low-temperature NH_3-SCR. *Chem. Eng. J.* **2013**, *228*, 815–823. [CrossRef]
34. Zhang, S.; Zhong, Q.; Zhao, W.; Li, Y. Surface characterization studies on F-doped V_2O_5/TiO_2 catalyst for NO reduction with NH_3 at low-temperature. *Chem. Eng. J.* **2014**, *253*, 207–216. [CrossRef]
35. Liang, Q.; Li, J.; He, H.; Yue, T.; Tong, L. Effects of SO_2 and H_2O on low-temperature NO conversion over F-V_2O_5-WO_3/TiO_2 catalysts. *J. Environ. Sci.* **2020**, *90*, 253–261. [CrossRef] [PubMed]

36. Yan, T.; Liu, Q.; Wang, S.; Xu, G.; Wu, M.; Chen, J.; Li, J. Promoter rather than inhibitor: Phosphorus incorporation accelerates the activity of V_2O_5-WO_3/TiO_2 catalyst for selective catalytic reduction of NO_x by NH_3. *ACS Catal.* **2020**, *10*, 2747–2753. [CrossRef]
37. Nam, K.B.; Yeo, J.H.; Hong, S.C. Study of the phosphorus deactivation effect and resistance of vanadium-based catalysts. *Ind. Eng. Chem. Res.* **2019**, *58*, 18930–18941. [CrossRef]
38. Putluru, S.S.R.; Schill, L.; Godiksen, A.; Poreddy, R.; Mossin, S.; Jensen, A.D.; Fehrmann, R. Promoted V_2O_5/TiO_2 catalysts for selective catalytic reduction of NO with NH_3 at low temperatures. *Appl. Catal. B* **2016**, *183*, 282–290. [CrossRef]
39. Bosch, F.J.H. Formation and control of nitrogen oxides. *Catal. Today* **1988**, *2*, 369–379.
40. Amiridis, M.D.; Duevel, R.V.; Wachs, I.E. The effect of metal oxide additives on the activity of V_2O_5/TiO_2 catalysts for the selective catalytic reduction of nitric oxide by ammonia. *Appl. Catal. B* **1999**, *20*, 111–122. [CrossRef]
41. Roy, S.; Hegde, M.S.; Madras, G.J.A.E. Catalysis for NO_x abatement. *Appl. Energy* **2009**, *86*, 2283–2297. [CrossRef]
42. Song, I.; Youn, S.; Lee, H.; Lee, S.G.; Cho, S.J.; Kim, D.H. Effects of microporous TiO_2 support on the catalytic and structural properties of V_2O_5/microporous TiO_2 for the selective catalytic reduction of NO by NH_3. *Appl. Catal. B* **2017**, *210*, 421–431. [CrossRef]
43. Youn, S.; Song, I.; Lee, H.; Cho, S.J.; Kim, D.H. Effect of pore structure of TiO_2 on the SO_2 poisoning over V_2O_5/TiO_2 catalysts for selective catalytic reduction of NO_x with NH_3. *Catal. Today* **2018**, *303*, 19–24. [CrossRef]
44. Liu, X.; Li, J.; Li, X.; Peng, Y.; Wang, H.; Jiang, X.; Wang, L. NH_3 selective catalytic reduction of NO: A large surface TiO_2 support and its promotion of V_2O_5 dispersion on the prepared catalyst. *Chin. J. Catal.* **2016**, *37*, 878–887. [CrossRef]
45. Tran, T.; Yu, J.; Gan, L.; Guo, F.; Phan, D.; Xu, G. Upgrading V_2O_5-WO_3/TiO_2 deNO_x catalyst with TiO_2-SiO_2 support prepared from Ti-bearing blast furnace slag. *Catalysts* **2016**, *6*, 56. [CrossRef]
46. Ferjani, W.; Boudali, L.K.; Delahay, G.; Petitto, C. Reduction of nitrogen oxide by ammonia over vanadium supported on mixed tungsten-titanium-pillared clays. *Chem. Lett.* **2016**, *45*, 872–874. [CrossRef]
47. Li, X.; Wu, Z.; Zeng, Y.; Han, J.; Zhang, S.; Zhong, Q. Reduced TiO_2 inducing highly active V_2O_5 species for selective catalytic reduction of NO by NH_3. *Chem. Phys. Lett.* **2020**, *750*, 137494. [CrossRef]
48. da Cunha, B.N.; Goncalves, A.M.; da Silveira, R.G.; Urquieta-Gonzalez, E.A.; Nunes, L.M. The influence of a silica pillar in lamellar tetratitanate for selective catalytic reduction of NO_x using NH_3. *Mater. Res. Bull.* **2015**, *61*, 124–129. [CrossRef]
49. Bukowski, A.; Schill, L.; Nietsen, D.; Mossin, S.; Riisager, A.; Albert, J. NH_3-SCR of NO with novel active, supported vanadium-containing Keggin-type heteropolyacid catalysts. *React. Chem. Eng.* **2020**, *5*, 935–948. [CrossRef]
50. Mejia-Centeno, I.; Castillo, S.; Camposeco, R.; Marin, J.; Garcia, L.A.; Fuentes, G.A. Activity and selectivity of V_2O_5/$H_2Ti_3O_7$, V_2O_5-WO_3/$H_2Ti_3O_7$ and Al_2O_3/$H_2Ti_3O_7$ model catalysts during the SCR-NO with NH_3. *Chem. Eng. J.* **2015**, *264*, 873–885. [CrossRef]
51. Cheng, J.; Song, Y.; Ye, Q.; Cheng, S.; Kang, T.; Dai, H. A mechanistic investigation on the selective catalytic reduction of NO with ammonia over the V-Ce/Ti-PILC catalysts. *Mol. Catal.* **2018**, *445*, 111–123. [CrossRef]
52. Vuong, T.H.; Radnik, J.; Rabeah, J.; Bentrup, U.; Schneider, M.; Atia, H.; Armbruster, U.; Grünert, W.; Brückner, A. Efficient VO_x/$Ce_{1-x}Ti_xO_2$ catalysts for low-temperature NH_3-SCR: Reaction mechanism and active sites assessed by in situ/operando spectroscopy. *ACS Catal.* **2017**, *7*, 1693–1705. [CrossRef]
53. Lian, Z.; Liu, F.; He, H. Effect of preparation methods on the activity of VO_x/CeO_2 catalysts for the selective catalytic reduction of NO_x with NH_3. *Catal. Sci. Technol.* **2015**, *5*, 389–396. [CrossRef]
54. Lian, Z.; Liu, F.; He, H. Enhanced activity of Ti-modified V_2O_5/CeO_2 catalyst for the selective catalytic reduction of NO_x with NH_3. *Ind. Eng. Chem. Res.* **2014**, *53*, 19506–19511. [CrossRef]
55. Lian, Z.; Liu, F.; He, H.; Liu, K. Nb-doped VO_x/CeO_2 catalyst for NH_3-SCR of NO_x at low temperatures. *RSC Adv.* **2015**, *5*, 37675–37681. [CrossRef]
56. Lian, Z.; Liu, F.; Shan, W.; He, H. Improvement of Nb doping on SO_2 resistance of VO_x/CeO_2 catalyst for the selective catalytic reduction of NO_x with NH_3. *J. Phys. Chem. C* **2017**, *121*, 7803–7809. [CrossRef]

57. Liu, S.; Wang, H.; Wei, Y.; Zhang, R.; Royer, S. Morphology-Oriented ZrO_2-Supported Vanadium Oxide for the NH_3-SCR Process: Importance of Structural and Textural Properties. *ACS Appl. Mater. Interfaces* **2019**, *11*, 22240–22254. [CrossRef]
58. Thanh Huyen, V.; Radnik, J.; Kondratenko, E.; Schneider, M.; Armbruster, U.; Brueckner, A. Structure-reactivity relationships in $VO_x/Ce_xZr_{1-x}O_2$ catalysts used for low-temperature NH_3-SCR of NO. *Appl. Catal. B* **2016**, *197*, 159–167.
59. Zhao, L.K.; Li, C.T.; Li, S.H.; Wang, Y.; Zhang, J.Y.; Wang, T.; Zeng, G.M. Simultaneous removal of elemental mercury and NO in simulated flue gas over V_2O_5/ZrO_2-CeO_2 catalyst. *Appl. Catal. B* **2016**, *198*, 420–430. [CrossRef]
60. Zhao, L.; Li, C.; Du, X.; Zeng, G.; Gao, L.; Zhai, Y.; Wang, T.; Zhang, J. Effect of Co addition on the performance and structure of V/ZrCe catalyst for simultaneous removal of NO and Hg^0 in simulated flue gas. *Appl. Surf. Sci.* **2018**, *437*, 390–399. [CrossRef]
61. Niu, C.; Wang, Y.; Ren, D.; Xiao, L.; Duan, R.; Wang, B.; Wang, X.; Xu, Y.; Li, Z.; Shi, J.W. The deposition of VWO_x on the $CuCeO_y$ microflower for the selective catalytic reduction of NO_x with NH_3 at low temperatures. *J. Colloid Interface Sci.* **2020**, *561*, 808–817. [CrossRef] [PubMed]
62. Keller, S.; Agostini, G.; Antoni, H.; Kreyenschulte, C.R.; Atia, H.; Rabeah, J.; Bentrup, U.; Brueckner, A. The effect of iron and vanadium in $VO_y/Ce_{1-x}Fe_xO_2$-delta catalysts in low-temperature selective catalytic reduction of NO_x by ammonia. *ChemCatChem* **2020**, *12*, 2440–2451. [CrossRef]
63. Bai, S.; Jiang, S.; Li, H.; Guan, Y. Carbon nanotubes loaded with vanadium oxide for reduction NO with NH_3 at low temperature. *Chin. J. Chem. Eng.* **2015**, *23*, 516–519. [CrossRef]
64. Bai, S.; Wang, Z.; Li, H.; Xu, X.; Liu, M. SO_2 promotion in NH_3-SCR reaction over V_2O_5/SiC catalyst at low temperature. *Fuel* **2017**, *194*, 36–41. [CrossRef]
65. Yang, W.; Liu, F.; Xie, L.; Lian, Z.; He, H. Effect of V_2O_5 additive on the SO_2 resistance of a Fe_2O_3/AC catalyst for NH_3-SCR of NO_x at low temperatures. *Ind. Eng. Chem. Res.* **2016**, *55*, 2677–2685. [CrossRef]
66. Jiang, L.; Liu, Q.; Ran, G.; Kong, M.; Ren, S.; Yang, J.; Li, J. V_2O_5-modified Mn-Ce/AC catalyst with high SO_2 tolerance for low-temperature NH_3-SCR of NO. *Chem. Eng. J.* **2019**, *370*, 810–821. [CrossRef]
67. He, Y.; Ford, M.E.; Zhu, M.; Liu, Q.; Tumuluri, U.; Wu, Z.; Wachs, I.E. Influence of catalyst synthesis method on selective catalytic reduction (SCR) of NO by NH_3 with V_2O_5-WO_3/TiO_2 catalysts. *Appl. Catal. B* **2016**, *193*, 141–150. [CrossRef]
68. Shen, M.; Xu, L.; Wang, J.; Li, C.; Wang, W.; Wang, J.; Zhai, Y. Effect of synthesis methods on activity of $V_2O_5/CeO_2/WO_3$-TiO_2 catalyst for selective catalytic reduction of NO_x with NH_3. *J. Rare Earths* **2016**, *34*, 259–267. [CrossRef]
69. Cha, W.; Ehrman, S.H.; Jurng, J. Surface phenomenon of CeO_2-added V_2O_5/TiO_2 catalyst based chemical vapor condensation (CVC) for enhanced selective catalytic reduction at low temperatures. *Chem. Eng. J.* **2016**, *304*, 72–78. [CrossRef]
70. Vuong, T.H.; Radnik, J.; Schneider, M.; Atia, H.; Armbruster, U.; Brückner, A. Effect of support synthesis methods on structure and performance of VO_x/CeO_2 catalysts in low-temperature NH_3-SCR of NO. *Catal. Commun.* **2016**, *84*, 171–174. [CrossRef]
71. Cheng, K.; Liu, J.; Zhao, Z.; Wei, Y.C.; Jiang, G.Y.; Duan, A.J. Direct synthesis of V-W-Ti nanoparticle catalysts for selective catalytic reduction of NO with NH_3. *RSC Adv.* **2015**, *5*, 45172–45183. [CrossRef]
72. Chen, T.; Lin, H.; Guan, B.; Gong, X.; Li, K.; Huang, Z. Promoting the low temperature activity of Ti-V-O catalysts by premixed flame synthesis. *Chem. Eng. J.* **2016**, *296*, 45–55. [CrossRef]
73. Song, I.; Lee, H.; Kim, D.H. Rotation-assisted hydrothermal synthesis of thermally stable multiwalled titanate nanotubes and their application to selective catalytic reduction of NO with NH_3. *ACS Appl. Mater. Interfaces* **2018**, *10*, 42249–42257. [CrossRef] [PubMed]
74. Doronkin, D.E.; Benzi, F.; Zheng, L.; Sharapa, D.I.; Amidani, L.; Studt, F.; Roesky, P.W.; Casapu, M.; Deutschmann, O.; Grunwaldt, J.D. NH_3-SCR over V-W/TiO_2 investigated by operando X-ray absorption and emission spectroscopy. *J. Phys. Chem. C* **2019**, *123*, 14338–14349. [CrossRef]
75. Gan, L.; Chen, J.; Peng, Y.; Yu, J.; Tran, T.; Li, K.; Wang, D.; Xu, G.; Li, J. NO_x removal over V_2O_5/WO_3-TiO_2 prepared by a grinding method: Influence of the precursor on vanadium dispersion. *Ind. Eng. Chem. Res.* **2018**, *57*, 150–157. [CrossRef]
76. Wang, H.; Wang, P.; Chen, X.; Wu, Z. Uniformly active phase loaded selective catalytic reduction catalysts (V_2O_5/TNTs) with superior alkaline resistance performance. *J. Hazard. Mater.* **2017**, *324*, 507–515. [CrossRef]

77. Casanova, M.; Nodari, L.; Sagar, A.; Schermanz, K.; Trovarelli, A. Preparation, characterization and NH_3-SCR activity of $FeVO_4$ supported on TiO_2-WO_3-SiO_2. *Appl. Catal. B* **2015**, *176–177*, 699–708. [CrossRef]
78. Liu, X.; Zhao, Z.; Ning, R.; Qin, Y.; Zhu, T.; Liu, F. Ce-doped V_2O_5-WO_3/TiO_2 with low vanadium loadings as SCR catalysts and the resistance of H_2O and SO_2. *Catal. Lett.* **2020**, *150*, 375–383. [CrossRef]
79. Chen, G.; Xu, J.; Yu, H.; Guo, F.; Xie, J.; Wang, Y. Effect of the non-thermal plasma treatment on the structure and SCR activity of vanadium-based catalysts. *Chem. Eng. J.* **2020**, *380*, 122286. [CrossRef]
80. Lian, Z.; Xin, S.; Zhu, N.; Wang, Q.; Xu, J.; Zhang, Y.; Shan, W.; He, H. Effect of treatment atmosphere on the vanadium species of V/TiO_2 catalysts for the selective catalytic reduction of NO_x with NH_3. *Catal. Sci. Technol.* **2020**, *10*, 311–314. [CrossRef]
81. Zhao, X.; Huang, L.; Li, H.R.; Hu, H.; Hu, X.N.; Shi, L.Y.; Zhang, D.S. Promotional effects of zirconium doped $CeVO_4$ for the low-temperature selective catalytic reduction of NO_x with NH_3. *Appl. Catal. B* **2016**, *183*, 269–281. [CrossRef]
82. Mu, J.; Li, X.; Sun, W.; Fan, S.; Wang, X.; Wang, L.; Qin, M.; Gan, G.; Yin, Z.; Zhang, D. Inductive Effect Boosting Catalytic Performance of Advanced $Fe_{1-x}V_xO_\delta$ Catalysts in Low-Temperature NH_3 Selective Catalytic Reduction: Insight into the Structure, Interaction, and Mechanisms. *ACS Catal.* **2018**, *8*, 6760–6774. [CrossRef]
83. Kim, J.; Kim, D.H.; Kwon, D.W.; Ha, H.P. Rational selection of $Fe_2V_4O_{13}$ over $FeVO_4$ as a preferred active site on Sb-promoted TiO_2 for catalytic NO_x reduction with NH_3. *Catal. Sci. Technol.* **2018**, *8*, 4774–4787. [CrossRef]
84. Marberger, A.; Elsener, M.; Ferri, D.; Sagar, A.; Schermanz, K.; Kroecher, O. Generation of NH_3 selective catalytic reduction active catalysts from decomposition of supported $FeVO_4$. *ACS Catal.* **2015**, *5*, 4180–4188. [CrossRef]
85. Wu, G.X.; Li, J.; Fang, Z.T.; Lan, L.; Wang, R.; Lin, T.; Gong, M.C.; Chen, Y.Q. Effectively enhance catalytic performance by adjusting pH during the synthesis of active components over $FeVO_4$/TiO_2-WO_3-SiO_2 monolith catalysts. *Chem. Eng. J.* **2015**, *271*, 1–13. [CrossRef]
86. Casanova, M.; Llorca, J.; Sagar, A.; Schermanz, K.; Trovarelli, A. Mixed iron-erbium vanadate NH_3-SCR catalysts. *Catal. Today* **2015**, *241*, 159–168. [CrossRef]
87. Gillot, S.; Tricot, G.; Vezin, H.; Dacquin, J.P.; Dujardin, C.; Granger, P. Development of stable and efficient $CeVO_4$ systems for the selective reduction of NO_x by ammonia: Structure-activity relationship. *Appl. Catal. B* **2017**, *218*, 338–348. [CrossRef]
88. Zhao, X.; Huang, L.; Namuangruk, S.; Hu, H.; Hu, X.N.; Shi, L.Y.; Zhang, D.S. Morphology-dependent performance of Zr-$CeVO_4$/TiO_2 for selective catalytic reduction of NO with NH_3. *Catal. Sci. Technol.* **2016**, *6*, 5543–5553. [CrossRef]
89. Gao, S.; Wang, P.; Yu, F.; Wang, H.; Wu, Z. Dual resistance to alkali metals and SO_2: Vanadium and cerium supported on sulfated zirconia as an efficient catalyst for NH_3-SCR. *Catal. Sci. Technol.* **2016**, *6*, 8148–8156. [CrossRef]
90. Huang, X.; Zhang, G.; Dong, F.; Tang, Z. The remarkable promotional effect of Sn on $CeVO_4$ catalyst for wide temperature NH_3-SCR process by citric acid-assisted solvothermal synthesis and post-hydrothermal treatment. *Catal. Sci. Technol.* **2018**, *8*, 5604–5615. [CrossRef]
91. Kim, J.; Kwon, D.W.; Lee, S.; Ha, H.P. Exploration of surface properties of Sb-promoted copper vanadate catalysts for selective catalytic reduction of NO_x by NH_3. *Appl. Catal. B* **2018**, *236*, 314–325. [CrossRef]
92. Kim, J.; Lee, S.; Kwon, D.W.; Lee, K.Y.; Ha, H.P. SO_3^{2-}/SO_4^{2-} functionalization-tailorable catalytic surface features of Sb-promoted $Cu_3V_2O_8$ on TiO_2 for selective catalytic reduction of NO_x with NH_3. *Appl. Catal. A* **2019**, *570*, 355–366. [CrossRef]
93. Gillot, S.; Tricot, G.; Vezin, H.; Dacquin, J.P.; Dujardin, C.; Granger, P. Induced effect of tungsten incorporation on the catalytic properties of $CeVO_4$ systems for the selective reduction of NO_x by ammonia. *Appl. Catal. B* **2018**, *234*, 318–328. [CrossRef]
94. Marberger, A.; Ferri, D.; Elsener, M.; Sagar, A.; Artner, C.; Schermanz, K.; Krocher, O. Relationship between structures and activities of supported metal vanadates for the selective catalytic reduction of NO by NH_3. *Appl. Catal. B* **2017**, *218*, 731–742. [CrossRef]
95. Wu, G.; Li, J.; Fang, Z.; Lan, L.; Wang, R.; Gong, M.; Chen, Y. $FeVO_4$ nanorods supported TiO_2 as a superior catalyst for NH_3-SCR reaction in a broad temperature range. *Catal. Commun.* **2015**, *64*, 75–79. [CrossRef]

96. Huang, X.; Zhang, G.; Tang, Z. Facile fabrication of Ce/V-modified multi-channel TiO_2 nanotubes and their enhanced selective catalytic reduction performance. *Chem. Asian J.* **2020**, *15*, 371–379. [CrossRef]
97. Lee, S.G.; Lee, H.J.; Song, I.; Youn, S.; Kim, D.H.; Cho, S.J. Suppressed N_2O formation during NH_3 selective catalytic reduction using vanadium on zeolitic microporous TiO_2. *Sci. Rep.* **2015**, *5*, 12702. [CrossRef]
98. Zhang, T.; Chang, H.; Li, K.; Peng, Y.; Li, X.; Li, J. Different exposed facets VO_x/CeO_2 catalysts for the selective catalytic reduction of NO with NH_3. *Chem. Eng. J.* **2018**, *349*, 184–191. [CrossRef]
99. Song, L.; Zhang, R.; Zang, S.; He, H.; Su, Y.; Qiu, W.; Sun, X. Activity of selective catalytic reduction of NO over V_2O_5/TiO_2 catalysts preferentially exposed anatase {001} and {101} facets. *Catal. Lett.* **2017**, *147*, 934–945. [CrossRef]
100. Boningari, T.; Pappas, D.K.; Smirniotis, P.G. Metal oxide-confined interweaved titania nanotubes M/TNT (M = Mn, Cu, Ce, Fe, V, Cr, and Co) for the selective catalytic reduction of NO_x in the presence of excess oxygen. *J. Catal.* **2018**, *365*, 320–333. [CrossRef]
101. Shan, W.; Song, H. Catalysts for the selective catalytic reduction of NO_x with NH_3 at low temperature. *Catal. Sci. Technol.* **2015**, *5*, 4280–4288. [CrossRef]
102. Forzatti, P. Present status and perspectives in de-NO_x SCR catalysis. *Appl. Catal. A* **2001**, *222*, 221–236. [CrossRef]
103. Shan, W.; Yu, Y.; Zhang, Y.; He, G.; Peng, Y.; Li, J.; He, H. Theory and practice of metal oxide catalyst design for the selective catalytic reduction of NO with NH_3. *Catal. Today* **2020**, in press.
104. Zhu, M.; Lai, J.K.; Tumuluri, U.; Wu, Z.; Wachs, I.E. Nature of active sites and surface intermediates during SCR of NO with NH_3 by supported V_2O_5-WO_3/TiO_2 catalysts. *J. Am. Chem. Soc.* **2017**, *139*, 15624–15627. [CrossRef]
105. Marberger, A.; Ferri, D.; Elsener, M.; Krocher, O. The significance of Lewis acid sites for the selective catalytic reduction of nitric oxide on vanadium-based catalysts. *Angew. Chem. Int. Ed.* **2016**, *55*, 11989–11994. [CrossRef]
106. Song, I.; Lee, H.; Jeon, S.W.; Kim, D.H. Understanding the dynamic behavior of acid sites on TiO_2-supported vanadia catalysts via operando DRIFTS under SCR-relevant conditions. *J. Catal.* **2020**, *382*, 269–279. [CrossRef]
107. Liu, H.; You, C.; Wang, H. Time-resolved in-situ IR and DFT study: NH_3 adsorption and redox cycle of acid site on vanadium-based catalysts for NO abatement via selective catalytic reduction. *Chem. Eng. J.* **2020**, *382*, 122756. [CrossRef]
108. Kong, M.; Liu, Q.; Jiang, L.; Tong, W.; Yang, J.; Ren, S.; Li, J.; Tian, Y. K^+ deactivation of V_2O_5-WO_3/TiO_2 catalyst during selective catalytic reduction of NO with NH_3: Effect of vanadium content. *Chem. Eng. J.* **2019**, *370*, 518–526. [CrossRef]
109. He, G.; Lian, Z.; Yu, Y.; Yang, Y.; Liu, K.; Shi, X.; Yan, Z.; Shan, W.; He, H. Polymeric vanadyl species determine the low-temperature activity of V-based catalysts for the SCR of NO_x with NH_3. *Sci. Adv.* **2018**, *4*, eaau4637. [CrossRef]
110. Jaegers, N.R.; Lai, J.K.; He, Y.; Walter, E.; Dixon, D.A.; Vasiliu, M.; Chen, Y.; Wang, C.; Hu, M.Y.; Mueller, K.T.; et al. Mechanism by which tungsten oxide promotes the activity of supported V_2O_5/TiO_2 catalysts for NO_x abatement: Structural effects revealed by V-51 MAS NMR spectroscopy. *Angew. Chem. Int. Ed.* **2019**, *58*, 12609–12616. [CrossRef]
111. Liu, K.; Yan, Z.; He, H.; Feng, Q.; Shan, W. The effects of H_2O on a vanadium-based catalyst for NH_3-SCR at low temperatures: A quantitative study of the reaction pathway and active sites. *Catal. Sci. Technol.* **2019**, *9*, 5593–5604. [CrossRef]